Title
1/2 MAGNETIZATION REVERSAL IN NUCLEATIQN CONTROLLED MAGNETS PART 1: THEORY

Authors
Ramesh, R.
Sriknshna, K.

Publication Date
1988-05-01

LBL-25094 1/2
Preprint

Lawrence Berkeley Laboratory
UNIVERSITY OF CALIFORNIA

Materials & Chemical Sciences Division

Submitted to Journal of Applied Physics

Magnetization Reversal in Nucleation Controlled Magnets Part I: Theory

R. Ramesh and K. Srikrishna

May 1988

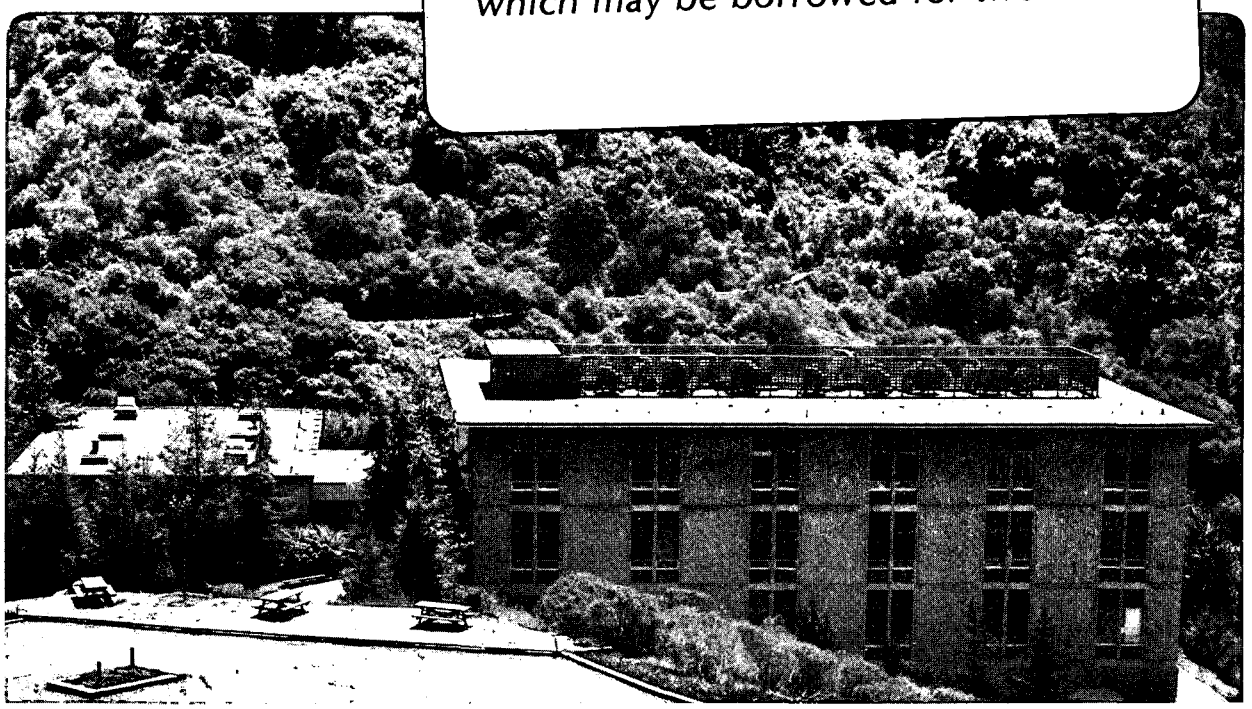

Prepared for the U.S. Department of Energy under Contract Number DE-AC03-76SF00098.

DISCLAIMER

Magnetization Reversal in Nucleation Controlled Magnets: Part I: Theory

R. Ramesh and K. Srikrishna , Department of Materials Science and Mineral Engineering and Materials and Chemical Sciences Division, Lawrence Berkeley Laboratory, University of California, Berkeley, CA 94720.

ABSTRACT : A statistical model, based upon earlier models of Brown(1962) and McIntyre(1970) has been developed to examine the magnetization reversal of domain wall nucleation controlled permanent magnets such as sintered Fe-Nd-B and $SmCo_5$. Using a Poisson distribution of the defects on the surface of the grains, a "weakest link statistics" type model has been developed. The model has been used to calculate hysteresis loops for sintered Fe-Nd-B type polycrystalline magnets. It is shown that the intrinsic coercivity measured for a bulk magnet should vary inversely as the logarithm of the surface area of the grain. The effect of demagnetizing field has been incorporated by a mean field type approximation, to calculate the overall nucleation field from the intrinsic coercivity. The hysteresis loops theoretically calculated are in excellent agreement with the overall form of those experimentally determined for similar nucleation controlled magnets. The model also predicts that for an inhomogeneous grain size distribution, such as a bi-modal distribution, kinks will be observed in the second quadrant of the hysteresis loop.

I. INTRODUCTION

Magnetization reversal in permanent magnets occurs by the nucleation and movement of magnetic domain walls, under the influence of a reverse magnetic field. In such permanent magnets, the important magnetic property is the intrinsic coercivity, iHc, and is never equal to the theoretically predicted value of anisotropy field, $H_A = 2K_1/M_s$, where K_1 is the first order anisotropy constant and M_s is the saturation magnetization of the magnet (Livingston 1987). Magnetization reversal (or deviation from saturation) occurs at fields much lower than the above predicted value. One of the main concerns in the design of permanent magnets is the achievement of high iHc values. In the case of magnets that reverse their magnetization by domain wall processes, high iHc can be achieved in either of two ways : (i) make the nucleation of a domain wall difficult ; (ii) make the movement of the wall through the grain difficult. These two methods lead naturally to two classes of technical permanent magnets : (i) corresponds to a "nucleation controlled" magnet , while (ii) corresponds to a "pinning controlled" magnet (Livingston 1987). In this paper the former aspect, i.e., the nucleation of domain walls in a "nucleation controlled" magnet will be addressed. It is thus implicitly assumed that once a domain wall is nucleated, magnetization reversal occurs almost instantaneously, i.e., there is no significant domain wall pinning in the volume of the magnet.

Conventionally, high iHc in nucleation controlled magnets has been achieved by using fine particles (Luborsky 1961). Such observations are not confined to any specific class of permanent magnets, and considerable information about the effect of particle size on the intrinsic coercivity and nucleation field is available (see, for example, the review by Wohlfarth(1959)). Furthermore, the iHc can be enhanced to values close to the anisotropy field by using whiskers or particles of size smaller than the critical size for single domain formation (DeBlois and Bean 1959). However, in practical permanent magnets, such as sintered Sm-Co and Fe-Nd-B magnets, the particle sizes (or grain sizes) are generally much larger than the critical size for single domain formation. The

tendency towards fine particles has been prompted by the inverse dependence of iHc on the particle (or grain) size. However, the exact nature of this inverse dependence has been an aspect of discussion. This will be one of the aspects that will be discussed in this paper.

The first treatment of the intrinsic coercivity of multi-domain particles was by Kittel(1949). He considered the balance between the wall formation energy, the energy of the wall in the external field and the self energy of the particle due to wall formation. The predictions of this model were in rough agreement with the experimental data of Guillaud (1949). Guillaud was one of the earliest researchers to determine the size dependence of the intrinsic coercivity, using Mn-Bi magnets. He observed an inverse dependence of the intrinsic coercivity on the particle size, although the relationship was not exactly hyperbolic. In contrast, Neel's model(Neel 1956), consisting of a cubic particle with internal and closure domain walls, predicted a $d^{-2/3}$ dependence of the intrinsic coercivity, where "d" is the particle size. However, quantitative agreement with experimental data was poor. Carey, Coleman and Viney (1972) have observed a "d^{-1}" dependence, similar to that observed by Guillaud (1949). There is a large amount of experimental data, such as the determination of hysteresis loops of particles of different sizes(Shur, Deryagin, Sisolina and Kandaurova 1970), available on this subject, and they are reviewed by Wohlfarth(1959). In recent years, in the case of sintered $SmCo_5$ magnets (which also behave predominantly as nucleation controlled magnets) McCurrie and Carswell(1971) and Becker(1968) have shown that the intrinsic coercivity decreases as the particle size increases. It was Brown(1962) who first suggested that the dependence of the intrinsic coercivity on the particle size could be related to the density of surface defects. Brown showed that if the number of defects in a surface area "S" is determined by a Poisson distribution, then the number of defects will decrease rapidly with grain size. Kandaurova, Deryagin and Lagutin (1975) have also suggested that the effect of particle size on the intrinsic

coercivity should be examined in terms of a statistical theory of wall nucleation. The model of Brown(1962) was further modified by McIntyre(1970) who obtained a relationship between the fraction of the magnet that had reversed its magnetization, under the applied reversing field, as a function of the grain size, and the reversing field. An important aspect of this model was that it predicted a "sigmoidal" shape for the plot of fraction unreversed against the applied field.

There is compelling evidence for the role of crystal defects in causing the nucleation of magnetization reversal(Aharoni 1962, Abraham and Aharoni 1960, Kronmuller and Hilzinger 1976, Kronmuller 1978 and Becker 1973). Buschow, Naastepad and Westendorp(1969) and Becker(1970) have shown that the intrinsic coercivity of $SmCo_5$ particles can be increased from 16.5kOe to 25kOe by etching in citric acid for 2 minutes, thus suggesting that the degree of imperfection of the surface of the particle has a marked influence on the intrinsic coercivity. Buschow et. al(1969) have shown that large increases in the intrinsic coercivity can be obtained by electroless nickel plating of the $SmCo_5$ particles, again suggesting modification of the defect configuration on the surface of the particles. Such defects could be voids, vacancies,grain boundaries, interphase interfaces (both coherent and incoherent), dislocations, etc.(Livingston 1973,1986) and defects can be introduced through any of the processing steps, or can be an inherent part of the crystal. In the neighbourhood of such regions, the magnetocrystalline anisotropy can be considerably lower than that in the matrix. So also, the magnetization and magnetostrictive properties of the crystal can be considerably modified. Such defects can be good sites for wall nucleation in high anisotropy permanent magnets. It is also clear that since a given particle can contain many defects, both in the volume and on the surface of the particle, the magnetic properties of the particle, specifically the nucleation field (the overall field at which a domain wall will nucleate to cause magnetization reversal) and the hysteresis properties, will be, to a large extent, statistical in character. This statistical nature is the focus of this paper. The

statistical model of Brown(1962), which was further improved upon by McIntyre(1970), will be used to explain the grain size dependence of the iHc of sintered Fe-Nd-B magnets. The model bears a strong similarity to the weakest link statistics used to interpret the fracture toughness of materials failing by cleavage fracture(Lin, Evans and Ritchie in press).

Based on the model theoretical hysteresis loops have been generated. There have been other models that have predicted the hysteresis loops of hard magnets. Jiles and Atherton(1986) have developed a mathematical model for the hysteresis loop, based upon the pinning of domain walls on defect sites. Escobar, Valenzuela and Magana(1983) have proposed a model for the magnetization curve and the hysteresis loop based on an irreversible domain wall displacement model. Using this model, they have obtained hysteresis loops which bear the general qualitative characteristics of the experimental loops. However, the fit, in terms of the actual shape and details of the hysteresis loop is not very close. One aspect of difference between these models and that of Brown(1962) and McIntyre(1970) is that these models are for the case of an already existent domain wall, that has to be unpinned from its pinned sites. In the case of the models of Brown(1962) and McIntyre(1970), however, the models predict magnetization reversal by wall nucleation. In their case, wall pinning in the volume of the magnet is not very important. This will be the approach in this paper.

II. STATISTICAL MODEL OF MAGNETIZATION REVERSAL

This model will consider the nucleation of reverse domains at defects in the material, specifically defects at the surface, grain boundaries and two phase interfaces. In the terminology of Brown[12], the 'extent', S will mean the surface area of the grain in question. Let a polyhedral grain, of size,'g' (which is, for example, the edge length measured from an optical micrograph), contain 'n' defects on its surface. Each of these defects possesses varying potency in terms of their ability to nucleate a domain wall. The exact nature of the defects is not determined,

although, as mentioned earlier, these defects could be impurity atoms at the grain boundaries, vacancies, stacking faults, dislocations, etc. The nucleation field for the reversal of magnetization of a given grain will correspond to the potency of the worst defect on the grain, i.e., the particle will 'fail' when the nucleation field of the 'weakest link' is attained. However, the distribution of defects on the surface of the grain and the dependence of the number of defects 'n' on the size of the grain is not transparent. Activation of any one of the 'n' defects is necessary and sufficient to cause the reversal. Thus, following the model of Brown(1962) and McIntyre(1970), it is assumed that the defects exist independently of one another(and do not influence one another), leading to a Poisson distribution of the number of defects 'n'. That is, the probability of finding "n" defects on a surface area "S" is given by :

$$P(n|S) = \exp(-\lambda.S).(\lambda.S)^n/n! \qquad (1)$$

where "λ" is a constant and is equal to the number of defects per unit area; S=the surface area of the grain under consideration. Also note that the average number of defects " $\bar{n}$ " is equal to $\lambda.S$. Therefore, " $\bar{n}$ ", the average number of defects, is proportional to the surface area of the grain.

The next step is to evaluate the distribution function of the nucleation fields for this grain. Let the nucleation field for any given flaw be "x", with a nucleation field distribution function, F(x). From the ideas of "weakest link statistics", i.e., the event "at least one nucleation field less than "x" " is exclusive to the event " all nucleation fields greater than "x"",
that is :

$$P(x_i < x) = F(x) \; ; \; P(x_i > x) = 1-F(x). \qquad (2)$$

Therefore, for "n" such sites,

$$P(\text{all } x_i > x|n) = \{1-F(x)\}^n. \qquad (3)$$

and hence

$$P(iHc < x|n) = 1- \{1-F(x)\}^n \quad (4)$$

where iHc is the intrinsic coercivity, i.e., the externally applied reverse field at which magnetization reversal occurs.

When the events are mutually exclusive events, the probability of occurrence of event A is given by the product of the probability of occurrence of event B, and the conditional probability of the occurrence of event A, given the event B. That is,

$$P(iHc < x) = \Sigma_n P(iHc\ x|n) . P(n) \quad (5)$$

This is the distribution function of the intrinsic coercivity, iHc and can be denoted by the function :

$$\Phi(iHc) = S_n[1- \{1-F(x)\}^n] . \exp(-\lambda.S) . (\lambda.S)^n/n! \quad (6)$$

By expanding terms in equation (6) it can be shown

$$\Phi(iHc) = 1-\exp\{-1.S.F(x)\} \quad (7)$$

This equation has the familiar form of a sigmoidal, which appears frequently in isothermal phase transformation kinetics[27]. Φ(iHc) is the cumulative fraction of the grain that has reversed its magnetization for a given coercive field of iHc. This idea is more relevant in the case of a polycrystalline magnet. In the case of a polycrystalline magnet:

$$\Phi\ (iHc) = Y(\text{grain size}, iHc) \quad (8)$$

For a given coercive field, iHc, Φ (iHc) is only a function of the grain size, ie

$$\Phi(iHc) = Y(\text{grain size}) \quad (9)$$

where Y defines the functional dependence. In the case where all the grains are of the same size, the magnet will behave similarly to a single particle. However, in the more realistic case of a polycrystalline magnet with a specific grain size distribution, e.g., normal or log-normal, the fraction reversed, Φ(iHc) will be a function of the grain size distribution also. It must be pointed out that although the magnet comprises many grains, the nucleation of magnetization reversal in each grain will be governed by the defect configuration on its surface only. That is, each grain, although in contact with other grains around it, will reverse at a field characteristic of the defect distribution on its surface, thus behaving as an isolated grain (from the point of view of defect induced domain wall nucleation). However, as will be shown later, in a polycrystalline magnet, magnetostatic interactions among the grains do exist and will influence the field at which reversal will occur. This aspect is discussed later.

In general, for powder metallurgy processed sintered magnets(Sagawa, Fujimura, Togawa, Yamamoto and Matsuura 1983), the grain size distribution is log-normal(Kolmogoroff 1941). This grain size distribution can be incorporated into **(7)** as follows : the grain size distribution is defined completely by the mean value, μ, and the standard deviation, σ. The frequency of each grain size in this distribution, ν_i ($0 < \nu_i < 1$) is determined by μ and σ.

In the case of a grain size distribution, Φ (iHc) = $\Sigma_i \nu_i \cdot Y(g_i)$, where g_i is a particular value of grain size. Thus, to evaluate Φ(iHc) at each value of iHc, the Φ(iHc) for each grain size in the distribution is first determined and then multiplied by the frequency of occurrence of that grain size, n_i.
That is,

$$\Phi \text{ (grain size, iHc)} = 1 - \exp\{-\lambda . S(\mu,\sigma) . F(x)\} \qquad \textbf{(10)}$$

In this equation, the effect of a grain size distribution has been incorporated by replacing the surface area term, S, with a modified surface area term that depends upon the mean and standard deviation of the grain size distribution.

In the above equation the following terms have to be defined : (a) the surface area, $S(\mu,\sigma)$: In the case of a spherical particle the surface area is given by $S = 4.\pi.r^2$, where r= the radius of the particle. However, in the case of real grains in a polycrystalline magnet, this approximation is not good enough. The shape of grains in a polycrystalline magnet can be approximated by that of a tetrakai- decahedron(German 1986). In that case, the surface area is given by: $S = 26.78.g^2$, where "g" is the edge length measured from an optical micrograph. Thus, the surface area is proportional to the square of the grain size measured off an optical micrograph. (b) Φ(iHc), the cumulative distribution function of the intrinsic coercivity: As described earlier, this is the fraction of the grains that have already reversed their magnetization for a given coercive field, iHc. This can be determined experimentally from the hysteresis loop, using the method suggested by McCurrie(1970). A typical hysteresis loop for a material such as Fe-Nd-B is shown schematically in Fig.1. In this figure, the demagnetizing curve depicts the magnetization remaining, along the initially applied field direction, as a function of the externally applied reversing field. In the completely saturated condition, (point L) all the grains are magnetized in the direction of the applied field. Upon reversal of the field direction, the grains progressively reverse their magnetization direction. From this demagnetization curve, LP, the distribution of intrinsic coercivities can be determined by obtaining the slope of the curve at fixed intervals on the curve. This value of the slope is an indicator of the fraction of grains that reverse their magnetization when the field is changed from iHc to iHc + dH. Normalizing each value of the slope by the sum of all the slopes gives the fraction of grains that have reversed for that field interval, dH. Φ_i is then obtained as the cumulative sum of all the fractions. This is the cumulative fraction of grains that have reversed for a given reverse field iHc. This fraction can be alternatively determined as a ratio of the instantaneous value of remnant magnetization to that of the saturated condition, i.e., at point L in Fig.1. This is the general method of determining the fraction of reversed grains.

(c) In the right hand side of equation **(10)** two terms, i.e., "λ" and F(x) remain undefined. In the absence of any analytical expressions to derive these two quantities, experimental results have to be resorted to. This is discussed in the next section.

III. DETERMINATION OF "λ" AND F(x)

As was mentioned earlier, equation **(9)** has the form of a sigmoidal. It can be rewritten as follows:

$$1- \Phi(\text{grain size, iHc}) = \exp\{-\lambda.S(\mu,s).F(x)\} \qquad \textbf{(11)}$$

i.e.,

$$\ln\{1-\Phi\} = -\lambda.S(\mu,\sigma).F(x) \qquad \textbf{(12)}$$

i.e.,

$$\ln[-\ln\{1-\Phi\}] = \ln[\lambda.S(\mu,\sigma)] + \ln[F(x)] \qquad \textbf{(13)}$$

Equation **(13)** suggests that a plot of the left hand side against ln[F(x)] must be a straight line with a slope that will be determined by the nature of the function F(x). It is also clear that the intercept of such a linear fit would give the value of "λ", if the plot is for a sample of known grain size and hence known value of "S". With this as the basis, a typical sintered magnet with an average grain size (experimentally determined) of 10μm was used to determine the hysteresis loop. The details of preparation of the magnets are given in the paper by Sagawa *et al.* (1983).

Fig.2 shows the measured grain size distribution for a typical sintered Fe-Nd-B magnet with an average grain size of 10 microns. The log-normal grain size distribution, with a positive skew is clearly demonstrated here. Fig.3 shows the experimental hysteresis loop for this sample, obtained with a maximum applied field of 25kOe. From this hysteresis loop, the intrinsic coercivity distribution, obtained using the method described in the previous paragraph, is shown in Fig.4, The plot of cumulative fraction of grains reversed against the applied reverse field is shown in Fig.5. Corresponding to this plot, Fig.6 shows a fit of ln[-ln{1-Φ}] against intrinsic coercivity, iHc. Several functional

forms of iHc, such $(iHc)^2$, $(iHc)^3$, etc were tried out and the best fit was obtained when plotted linearly. From this result two aspects became apparent. The first is the nature of the function F(x). The nature of the fit in Fig.6 clearly shows that F(x) is of the form $F(x) = \exp(-k.iHc)$, where "k" is the constant of proportionality, that can be determined from the linear fit in Fig.6. The second point is that the intercept of this linear fit provides a value for $\ln(\lambda.S)$. With the assumption that the average grain size of 10μm is representative of the whole sample (so that the grain size distribution can be replaced by a single average grain size), the value of "λ" can be determined, since "S" is related to the grain size "g" through the equation : $S = 26.78.g^2$. It should be pointed out that this value of "λ" is averaged over several grain sizes, represented by the average grain size.

Effect of demagnetizing fields

In the case of dense, polycrystalline sintered magnets, the interaction of grains with one another is another important factor to be taken into account, when examining the magnetization reversal characteristics of the magnet as a whole. While the presence of impurities and non-magnetic phases at grain boundaries(Ramesh, Chen and Thomas 1987) (in the case of Fe-Nd-B magnets), may prevent significant exchange interaction across the grain boundaries, there is bound to be significant magnetostatic interaction between the grains. Thus, demagnetizing fields have to be included in the calculation of the nucleation field. In general, the nucleation field has two contributions : (i) the external reversing field, which is the experimentally measured intrinsic coercivity, iHc ; (ii) the internal demagnetizing field. Thus, the nucleation field, i.e., the overall field under which the grain undergoes reveral of magnetization, can be written down as(Hirosawa, Tokuhara, Matsuura, Yamamoto, Fujimura and Sagawa 1986 and Herzer, Fernengel and Adler 1986):

$$H_n = iHc + D.M_S \qquad (14)$$

where D is the demagnetizing factor, which is geometry dependent, and M_S is the saturation magnetization. Thus, the grain undergoes

magnetization reversal when the overall field is equal to or greater than the nucleation field of the worst defect. In the case of a polycrystalline magnet undergoing reversal, however, the demagnetizing field, changes continuously as the whole magnet reverses its magnetization direction. This is schematically depicted in Figs.7(a-e). In Fig.7(a), the polycrystalline magnet is shown, magnetized in the direction of the initially applied field. The demagnetizing field in this case is equal to the $D.M_S$. In (b), the state of the magnet at the remanence point (see Fig.1) is shown. In this case, a small fraction of the grains, (predominantly those at the surface of the sample) have reversed their magnetization. However, this changes the demagnetizing field that a grain that has still not reversed, experiences. The demagnetizing field on a grain that has not reversed its magnetization will now be the sum of the demagnetizing field due to its own magnetization and the effective field (in a mean field type of approximation)of all the grains around it that have either reversed or are still unreversed. This additional contribution will be proportional to the instantaneous value of magnetization of the magnet, since the instantaneous value of magnetization is a measure of the number of grains that have reversed. Thus, the effective demagnetizing field at any point on the hysteresis loop is equal to $D.(M_S + [M_S-M_{inst.}])$, where $M_{inst.}$ is the instantaneous value of magnetization. The value of $D.M_S$ will be assumed to be equal to $I_S=4\pi.M_S$ (which is generally about 12.5-13 kGauss for Fe-Nd-B magnets at room temperature), since the value of "D" could not be determined accurately. As the reversing field increases in magnitude, the effective demagnetizing field on a grain that has still not reversed, increases. For example, at the coercive point, Fig.7(c), i.e., at the point where the effective magnetization is zero, the effective demagnetizing field is equal to $2.I_S$. In the extreme case where all but one grain has reversed (i.e., at very large negative fields),Fig.7(e), the effective demagnetizing field will be equal to $I_S + [I_S -(-I_S)]$, i.e., $3.I_S$. Fig.6, showing the linear fit between $\ln[-\ln(1-\Phi)]$ and iHc, can also be plotted between $\ln[-\ln(1-\Phi)]$ and H_n, the nucleation field, defined by

eqn.**(14)**. This plot is shown in Fig.8, and again, a linear fit is obtained. Since the nucleation field is a more relevant parameter (wall nucleation occurs when H_N is equal to the nucleation field of the worst defect), all the computations were carried out for the nucleation field. The values of "λ" and "k" used were those determined from Fig.8.

IV. ANALYTICAL RESULTS

The theory outlined above was incorporated into a simple computer program and B - H loops were generated for various grain distributions. Primarily three kind of grain configurations were simulated: single size grains(i.e., grain size distribution is a delta function at the mean value), unimodal distribution and a bimodal distribution of grains. The unimodal and bimodal distributions were both log normal in nature as these are the most commonly observed distributions in powder metallurgy processed sintered magnets. In all the cases, the simulations were carried out for the nucleation field and hence the corresponding values of "λ" and "k" (from Fig.8) were used in the calculations. The grain sizes were sampled from 0 to $\ln(g_{max})$ microns where g_{max} was such that the area under the grain size distribution curve included 99% of the grains. The value of "λ" was assumed to be independent of the grain size.

Figure 9 shows the calculated hysteresis loop for a single grain size (10 μm) polycrystalline magnet of Fe-Nd-B, and for a polycrystalline magnet with a grain size distribution as shown in Fig.10. The hysteresis loop for the magnet with a grain size distribution as in Fig.10 shows remarkable agreement with the general form of those experimentally determined. One feature of this plot to be noticed is the abrupt nature of the demagnetizing curve at the ends, in the case of the sample with only one grain size. It can also be seen that the slope of the demagnetizing curve in this case is different from that of the magnet with the grain size distribution shown in Fig.10. This difference can be directly attributed to the fact that in the case of the sample with the

grain size distribution as in Fig.10, grains larger and smaller than 10μm exist along with a lower fraction of grains of 10μm size. Because of this, the slope of the hysteresis loop in the initial stage as well as at the end, is different. So also, the nucleation field, $H_{0.5}$, is also lower in the case of the sample with the grain size distribution, compared to the sample with only 10μm grains.

Uni-modal grain size distributions: The simulated figures and the observed changes therein can be easily explained. The different stages in the demagnetization process of a polycrystalline magnet are shown in Fig.7(a-e). In (a) the magnet is completely saturated along the initially applied field direction and hence all the grains are magnetized in the same direction. As the positive field is decreased, nucleation of reverse domains occurs. This nucleation is primarily defect controlled and therefore the larger grains possesing greater surface area and hence a greater probability of finding a "bad" defect (i.e., one that can easily cause the nucleation of reverse domains) reverse first. Traversing the grain size distribution curve (such as in figure 10), with decreasing field, the reversal gradually increases till the average grain size is reached when the majority of the grains reverse. On further increase (i.e., increasing negative fields) of demagnetizing field the remaining grains smaller than the average grain size reverse.

The predicted behaviour of the hysteresis loop on increasing the standard deviation for a given grain size can also be explained based on similar arguments. Figures 11 and 12 depict the calculated grain size distributions and the corresponding hysteresis loops for Fe-Nd-B magnets of a given average grain size with varying standard deviations. Such changes in the grain size distribution can be achieved by suitable modification of the processing parameters. With increasing standard deviation the peak height decreases and consequently the number of grains having grain sizes greater and smaller than the average increases. As can be seen this causes a change in slope of the B-H loop at both extremums, as an increased fraction of grains transform sooner (the

large grains) and an increased fraction transform later (small grains). Since the fraction of grains with the average value decreases with increase in the standard deviation, the nucleation field, $H_{0.5}$, also decreases.

Of greater significance is the effect of average grain size, μ, on the hysteresis loop, for a constant value of the standard deviation, σ. This is shown in Figs.13 and 14. In Fig.13 the grain size distribution for three different average grain sizes, namely, 10, 20 and 40 microns, are plotted, for a constant value of the standard deviation of 0.4. The corresponding hysteresis loops are depicted in Fig.14. The main effect of increasing the grain size is a reduction in the width of the hysteresis loops. Consequently, and as expected, the nucleation field, i.e., $H_{0.5}$, also decreases with increase in grain size, an observation in consonance with experimental results.

Bi-modal grain size distributions: Frequently, inhomogeneous grain size distributions can be obtained in sintered magnets, if the sintering conditions are not properly controlled. For example, if the sintering temperature is higher than that required, inhomogeneous grain growth can occur. Under such conditions, grains whose sizes are an order or two larger than that of the rest of the magnet, can be observed. The presence of such an inhomogeneous grain size distribution can produce distinct effects upon the hysteresis loop. This inhomogeneous grain size distribution can be modeled by a bi-modal grain size distribution. Such a bi-modal distribution (on the log scale) would consist of a large fraction of the grains of small average size and a small fraction of grains of large size. Fig.15 is a hysteresis loop obtained for a uni-modal grain size distribution with an average size of 10 microns and a standard deviation of 0.2. Superimposed on this is the hysteresis loop for a bi-modal grain size distribution, consisting of 80% of 10 micron average grain size grains and 20% of 100 micron average size grains. In the case of a bi-modal grain size distribution, a kink appears in the second quadrant of the hysteresis loop(and in the fourth quadrant). Upon closer

examination of the hysteresis loops in Fig.15 it is clear that the deviation from saturation occurs at positive field and continues until about 20% of the magnet has transformed, i.e., all the large grains have reversed. After this stage, the loop follows that of the 10 micron sample, indicating that all the grains in the 100 micron fraction have already reversed their magnetization. This clearly shows that an inhomogeneous grain size distribution can lead to kinks in the hysteresis loop, with the location of the kink (or abrupt deviation from saturation) being dependent upon the size of the large grains. The magnitude of the kink, i.e., the drop in magnetization, is proportional to the fraction of large grains. This is illustrated by the plots in Figs.16 & 17. Fig.16 shows three typical examples of bi-modal grain size distributions. In this case, the two grain sizes chosen are 10 microns and 100 microns, with a standard deviation of 0.2 for each. The figure shows three plots, for different fractions of the 100 microns average size grains, i.e., 10, 20 and 30 vol.%. In reality, such large fractions of the large grains may not exist, but the examples chosen do clearly illustrate the point. The hysteresis loops corresponding to the three grain size distributions in Fig.16, are shown in Fig.17. All the hysteresis loops show deviation from saturation at the same value of the demagnetizing field, i.e., about +30kOe. However, the magnitude of the kink increases with increase in the fraction of the large grains. Experimental results confirming these theoretical inferences will be presented in the companion paper.

V. DISCUSSION

In this paper, a statistical model, based upon the earlier models of Brown(1962) and McIntyre(1970) has been developed to examine the magnetization reversal behaviour of domain wall nucleation controlled magnets, such as sintered Fe-Nd-B and $SmCo_5$. One of the most important features of this model is that sigmoidal hysteresis loops are obtained through an analysis similar to that frequently encountered in solid state phase transformations (Christian 1975). Using experimentally measured hysteresis loops

for a sample of known grain size and grain size distribution, it has been possible to determine the nature of the function F(x), the nucleation field distribution function. Instead of a power law type dependence (as in soild state phase transformations), the form of this function has been determined to be an exponential. In addition, the model suggests a possible method of evaluating the effect of average grain size on the intrinsic coercivity measured experimentally. This can be achieved by examining equation **(10)**. The intrinsic coercivity of a polycrystalline sintered magnet, as measured, is the median value of the distribution of coercivities of the collection of particles in the magnet. This median value is the value of the reverse field which reduces the effective magnetization to zero (i.e., the intercept on the negative x-axis of the second quadrant hysteresis loop). In this condition, exactly half of the grains in the magnet have reversed their magnetization, whence $\Phi = 0.5$. Using this value of Φ in eqn. **(10)**, we obtain :

$$0.5 = 1-\exp\{-\lambda.S(\mu,\sigma).F(x)\} \qquad \textbf{(15)}$$

i.e.,

$$0.5 = \exp\{-\lambda.S(\mu,\sigma).F(x) \qquad \textbf{(16)}$$

i.e.,

$$F(iHc) = \ln(2)/(\lambda.S) \qquad \textbf{(17)}$$

Eqn. **(17)** can be used to establish the relationship between the macroscopic average grain size of the magnet. "S" is the surface area of the grains. For an average grain size of "g":

$$S = 26.78.\ g^2 \qquad \textbf{(18)}$$

Thus,

$$F(iHc) = \ln(2)/(\lambda.\ 26.78.\ g^2) \qquad \textbf{(19)}$$

Since F(iHc) has been determined to be of the form $F(iHc) = \exp(k.iHc)$, the relationship between the macroscopically measured intrinsic coercivity, iHc, and the macroscopic average grain size, "g", can be established.

$$\exp(k.iHc) = \ln(2)/(\lambda.\ 26.78.g^2) \qquad (20)$$

Upon taking logarithms on both sides, one obtains :

$$k.iHc = \ln[\ln(2)] - \ln[\lambda.\ 26.78.g^2] \qquad (21)$$

Thus, the model predicts an inverse logarithmic relationship between the intrinsic coercivity and the average number of defects, $(\lambda.S)$, on the surface of the grains constituting the magnet. This dependence on the number of defects may be taken as an indication that as the number of defects increases, the probability of finding a "bad" defect with a very low nucleation field, increases. Since the average number of defects is related to the surface area, S, of the grain, the intrinsic coercivity is related to the surface area of the grain. This is turn means that the intrinsic coercivity is related to the average grain size of the magnet. The experimental verification of this model is presented in the companion paper.

The theoretical hysteresis loops generated by the computer program bear close resemblance to experimentally determined hysteresis loops for sintered polycrystalline nucleation controlled magnets. The model also predicts that if the magnet consists of an inhomogeneous grain size distribution, such as a bi-modal distribution, then kinks would be observed in the second quadrant of the hysteresis loops. This suggests that, in addition to the effect of spin reorientation at low temperatures, and the effect of oxidation and the presence of a soft magnetic phase, an inhomogeneous grain size distribution can also produce kinks in the hysteresis loops. Experimental verification of this prediction is presented in the companion paper.

VI. CONCLUSIONS

A statistical model to explain magnetization reversal by domain wall nucleation at crystal defects has been developed, based upon earlier models of Brown and McIntyre. Using a Poisson distribution

of the defects on the surface (i.e., grain surface nucleation) a "weakest link statistics" type model has been developed. The model has been employed to calculate hysteresis loops for Fe-Nd-B type sintered polycrystalline nucleation controlled magnets. It is shown that the intrinsic coercivity measured for a bulk magnet should vary inversely as the logarithm of the surface area of the grain. A mean field type approximation has been used to incorporate the effect of demagnetizing field and to calculate the overall nucleation field from the intrinsic coercivity. The hysteresis loops theoretically calculated are in excellent agreement with the overall form of experimental hysteresis loops for similar nucleation controlled magnets. The model also predicts that for an inhomogeneous grain size distribution, such as a bi-modal grain size distribution, kinks will be observed in the second quadrant of the hysteresis loop. Detailed experimental verification of the predictions of the model follows in the companion paper.

ACKNOWLEDGEMENTS: The authors wish to acknowledge the continued support and encouragement of Professor G.Thomas and stimulating discussions with Dr.R.M.Cannon, C.Carter and M.Sluiter during the course of this research. This work was supported by the Director, Office of Energy Research, Office of Basic Energy Sciences, Materials Sciences Division of the U.S. Department of Energy under contract No. DE-AC03-76SF00098.

REFERENCES

C.Abraham and A.Aharoni, Phys. Rev., 120, 1576(1960).

A.Aharoni, Rev. of Modern Physics, 34, 227(1962).

J.J.Becker, Jl. of Appl. Phys., 39, 1270(1968).

J.J.Becker, IEEE Trans. on Magnetics, MAG.-5, 211(1969) ; Jl. of Appl. Phys., 41, 1055(1970).

J.J.Becker, IEEE Trans. on Magn., MAG.-9, 161(1973).

W.F.Brown, Jr., Jl. of Appl. Phys., 33, 3022-3025(1962).

K.H.J.Buschow, P.A.Naastepad and F.F.Westendorp, Jl. of Appl. Phys., 40, 4029(1969).

R.Carey, J.E.Coleman and I.V.F.Viney, Proc. Royal Soc. of London, 328A, 143-151(1972).

J.W.Christian, Theory of Transformations in Metals and Alloys, Pergamon Press, (1975).

R.W.DeBlois and C.P.Bean, Jl. of Appl. Phys., 30, 225S(1959).

M.A.Escobar, R.Valenzuela and L.F.Magana, Jl. of Appl. Phys., 54, 5935-5940(1983).

R.M.German, The Int. Jl. of Powder Metallurgy, 22, 31(1986).

C.Guillaud, Jl.Rech. C.N.R.S., 2, 267-278(1949).

G.Herzer, W.Fernengel and E.Adler, Jl. of Magn. and Mag. Matls., 58, 48(1986).

S.Hirosawa, K.Tokuhara, Y.Matsuura, H.Yamamoto, S.Fujimura and M.Sagawa, Jl. of Magn. and Mag. Matls., 61, 363(1986).

D.C.Jiles and D.L.Atherton, Jl. of Magn. and Mag. Matls., 61, 48-60(1986).

G.S.Kandaurova, A.V.Deryagin and A.E.Lagutin, Phys. Stat. Sol. 27A, 429(1975).

C.Kittel, Rev. of Mod. Phys., 21, 541-583(1949).

A.N.Kolmogoroff, Dokl. Acad. Nauk SSSR,31, 999(1941).

H.Kronmuller and H.R.Hilzinger, Jl. of Magnetism and Magnetic Materials, 2, 3(1976).

H.Kronmuller, Jl. of Magn. and Mag. Matls., 7, 341(1978).

T.Lin, A.G.Evans and R.O.Ritchie, Met. Trans. (in Press).

J.D.Livingston, AIP Conf. Proc. 10, 643(1973).

J.D.Livingston, in Proc. ASM Symposium on Soft and Hard

Magnetic Materials, Ed.J.A.Salsgiver et. al., ASM Materials Week'86, Lake Buena Vista, Florida, 4-9 October, 1986.

J.D.Livingston, Paper No. AC-06, Intermag-1987, Tokyo, April 14-17, 1987.

F.E.Luborsky, Jl. of Appl. Phys., 32S, 171(1961).

R.A.McCurrie, Phil. Mag., 22, 1013(1970).

R.A.McCurrie and G.P.Carswell, Phil. Mag.,23, 333(1971).

D.A.McIntyre, Jl. of Physics, D3, 1430(1970).

L.Neel, Jl. Phys. Radium, 17, 250-255(1956).

R.Ramesh, J.K.Chen and G.Thomas, Jl. of Appl. Phys., 61, 2993(1987).

M.Sagawa, S.Fujimura, N.Togawa, H.Yamamoto and Y.Matsuura, Jl. of Appl. Phys., 55,2083(1983).

J.S.Shur, A.V.Deryagin, T.V.Sisolina and G.S.Kandaurova, Fiz. Metallov. Metallovidenie, 30, 908-914(1970).

E.P.Wohlfarth, Advances in Physics, 8, 87-224(1959).

FIGURE CAPTIONS

Figure 1 : Schematic representation of the typical virgin curve and hysteresis loop for an optimally treated sintered Fe-Nd-B magnet.

Figure 2 : Grain size distribution for a typical optimally treated, sintered Fe-Nd-B magnet, with an average grain size of about 10 microns.(Nominal composition of magnet: Fe-35wt.%Nd-1wt.%B).

Figure 3 : Experimental virgin curve and hysteresis loop for the magnet with grain size distribution shown in Fig.2. (Maximum applied field = 25kOe).

Figure 4 ; Intrinsic coercivity distribution for the magnet with grain size distribution in Fig.2, obtained from the hysteresis loop in Fig.3.

Figure 5 : A plot of cumulative fraction of grains reversed against the applied reverse field, obtained from Fig.4.

Figure 6 : A plot of ln[-ln(fraction unreversed)] against intrinsic coercivity, iHc, showing a linear fit, with a regression coefficient of 0.99

Figure 7 : Schematic representation of the grains in the polycrystalline magnet, undergoing magnetization reversal, as a function of the applied reverse field. (a) magnet saturated in the direction of the applied field ; (b) state of the magnet at the remanence point, with the magnetization of a small fraction of the grains reversed ; (c) state of the magnet at the coercive point, i.e., the effective magnetization is zero ; (d) state of the magnet with the magnetization of more than half of the grains reversed ; (e) state of the magnet in a very large reversing field, when the magnetization of all but a few of the grains has reversed.

Figure 8 : A plot of ln[-ln(fraction unreversed)] against the nucleation field, H_N. Note the linear fit with a regression coefficient of 1.0.

Figure 9 : Calculated hysteresis loop for a magnet with a uniform grain size of 10 microns and a magnet with grain size distribution as shown in Fig.10. The constants "λ" and "k" used were those obtained from Fig.8.

Figure 10: Calculated grain size distribution for an average grain size of 10 microns and a standard deviation of 0.2, used to calculate the theoretical hysteresis loop in Figure 9.

Figure 11: Theoretical grain size distributions for magnets with the same average grain size but with different standard deviations in the distribution.

Figure 12: Theoretical hysteresis loops for the grain size distributions shown in Figure 11.

Figure 13: Theoretical grain size distributions for magnets with different average grain sizes, but with the same standard deviation for the distribution.

Figure 14: Calculated hysteresis loops for the magnets with different average grain sizes, illustrated in Figure 13.

Figure 15: Calculated hysteresis loop for a magnet with average grain size of 10 microns and standard deviation of 0.2, with a uni-modal grain size distribution and for a magnet with a bi-modal grain size distribution. The magnet with a bi-modal distribution consists of 80% of grains with an average size 10 microns and standard deviation of 0.2, and 20% of grains with an average size of 100 microns and standard deviation of 0.2.

Figure 16: Bi-modal grain size distributions with average sizes of 10 microns and 100 microns for three values of the fraction of large grains, i.e., 10%, 20% and 30%.

Figure 17: Calculated hysteresis loops for the three samples shown in Figure 16.

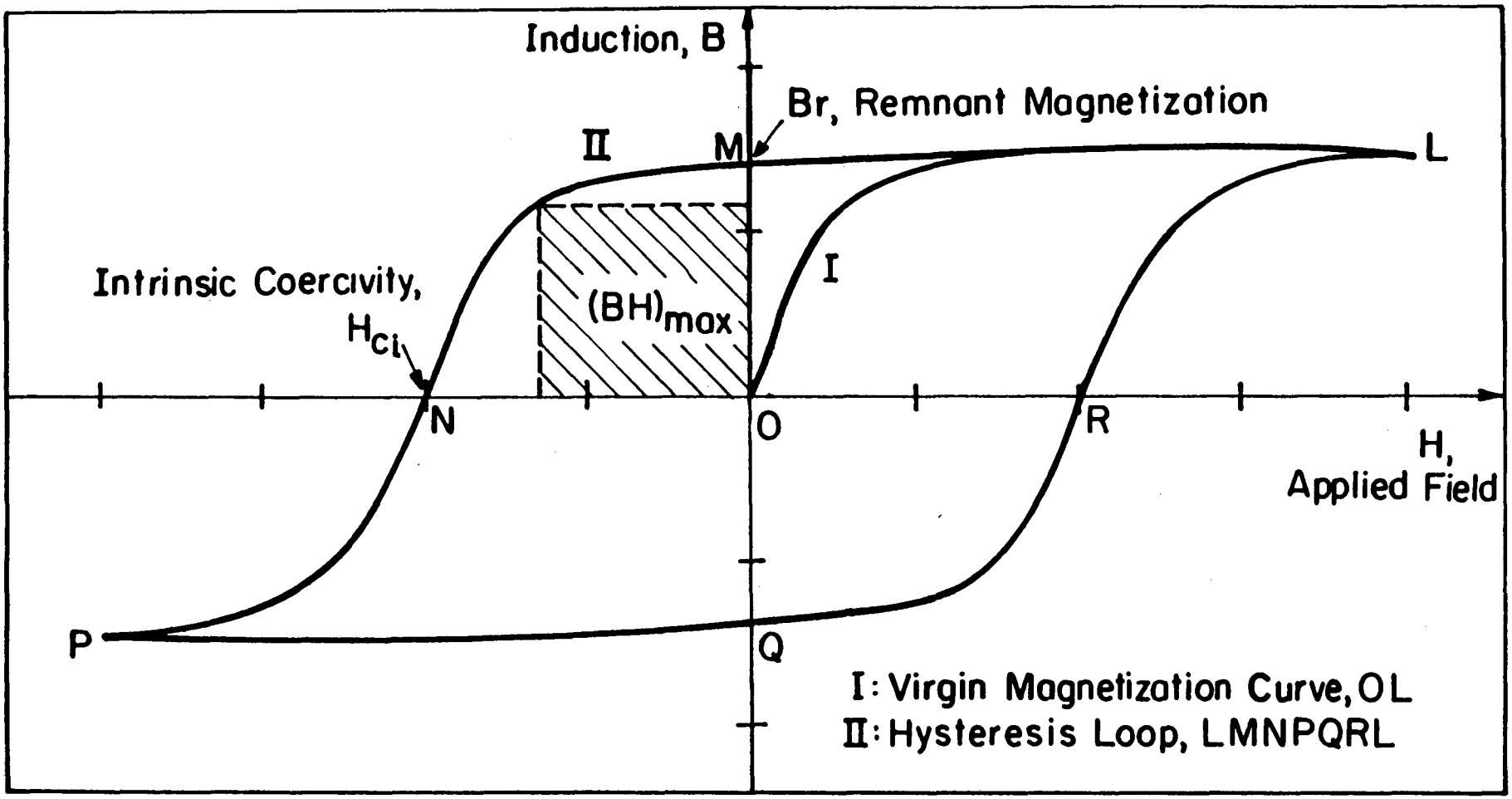

XBL8512-6870

Figure I

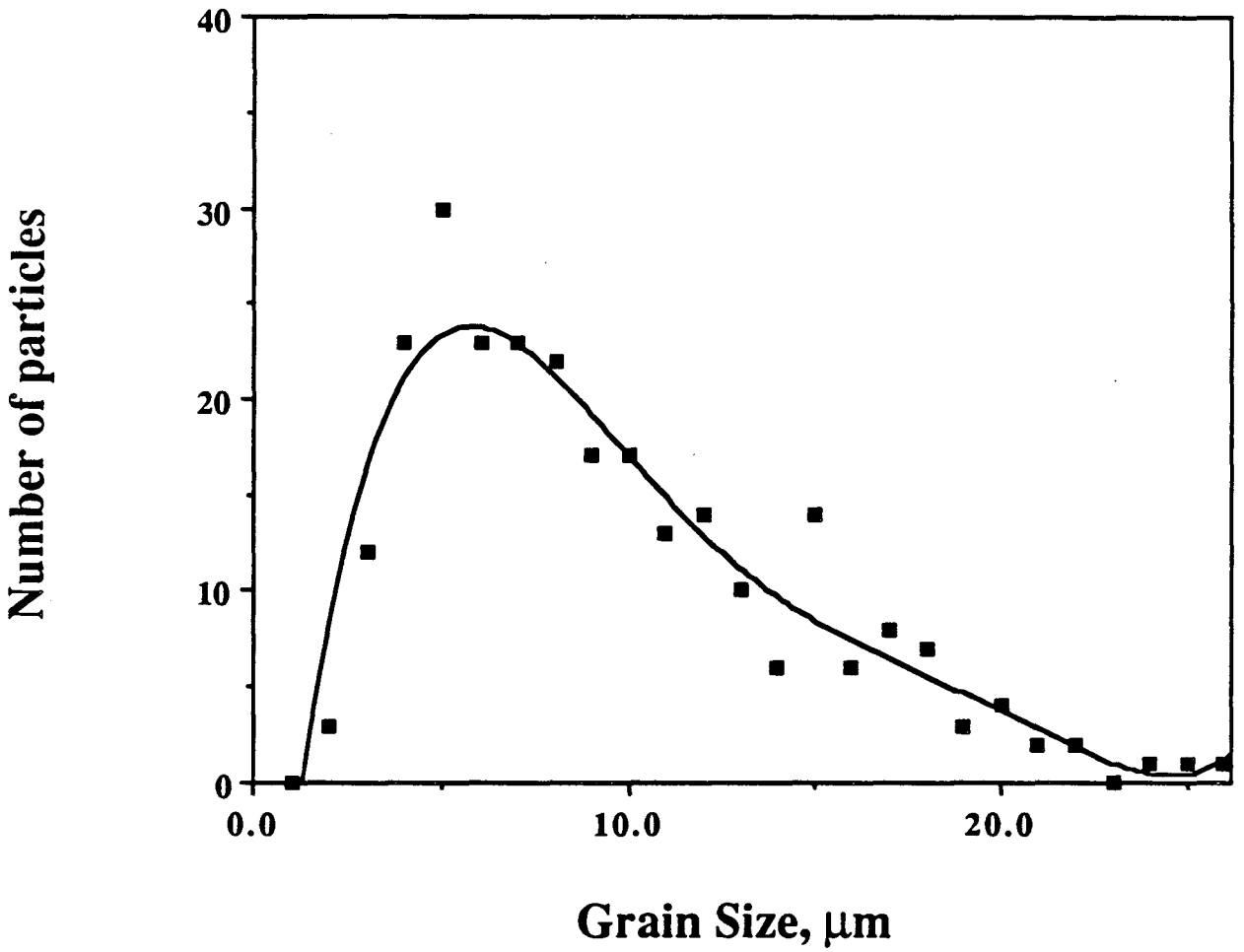

-- XBL 877-3382 --

Figure 2

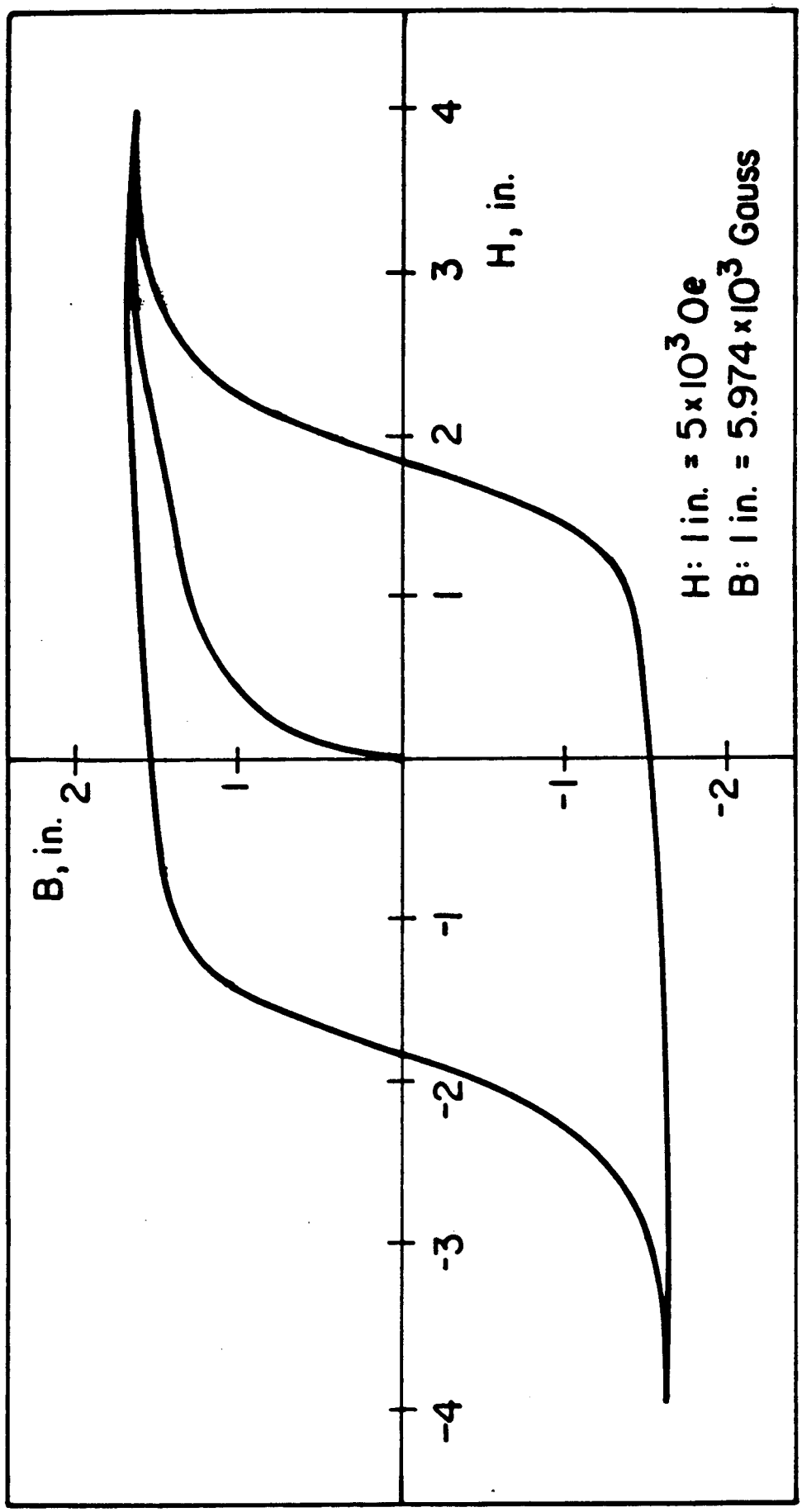

Figure 3

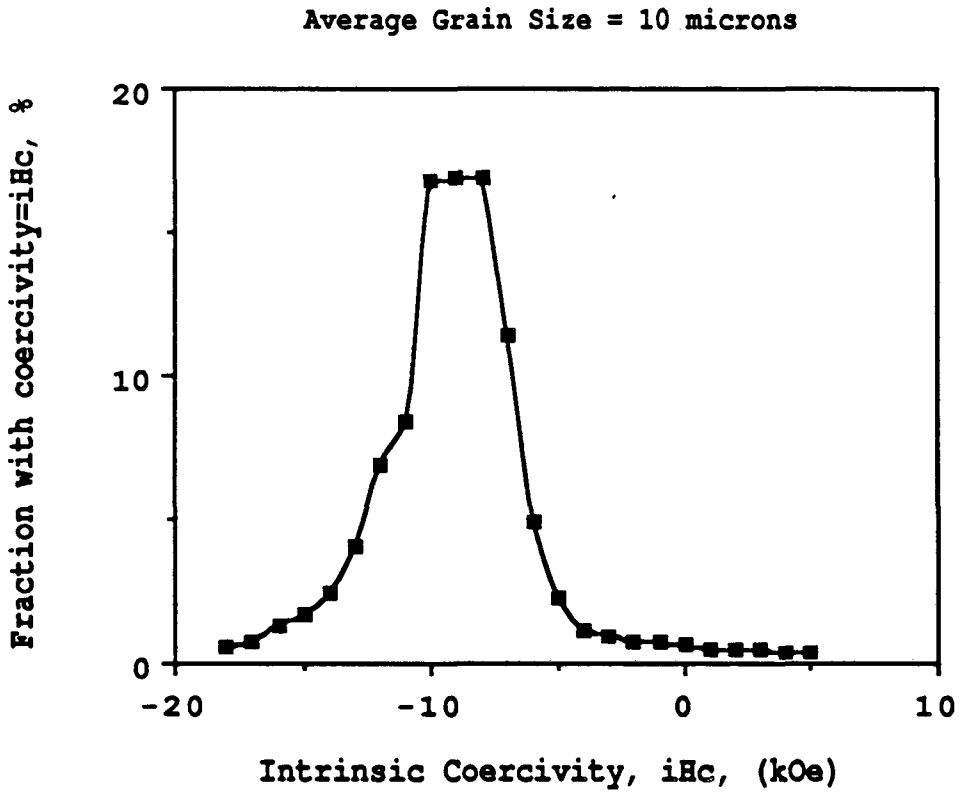

XBL 885-1550

Figure 4

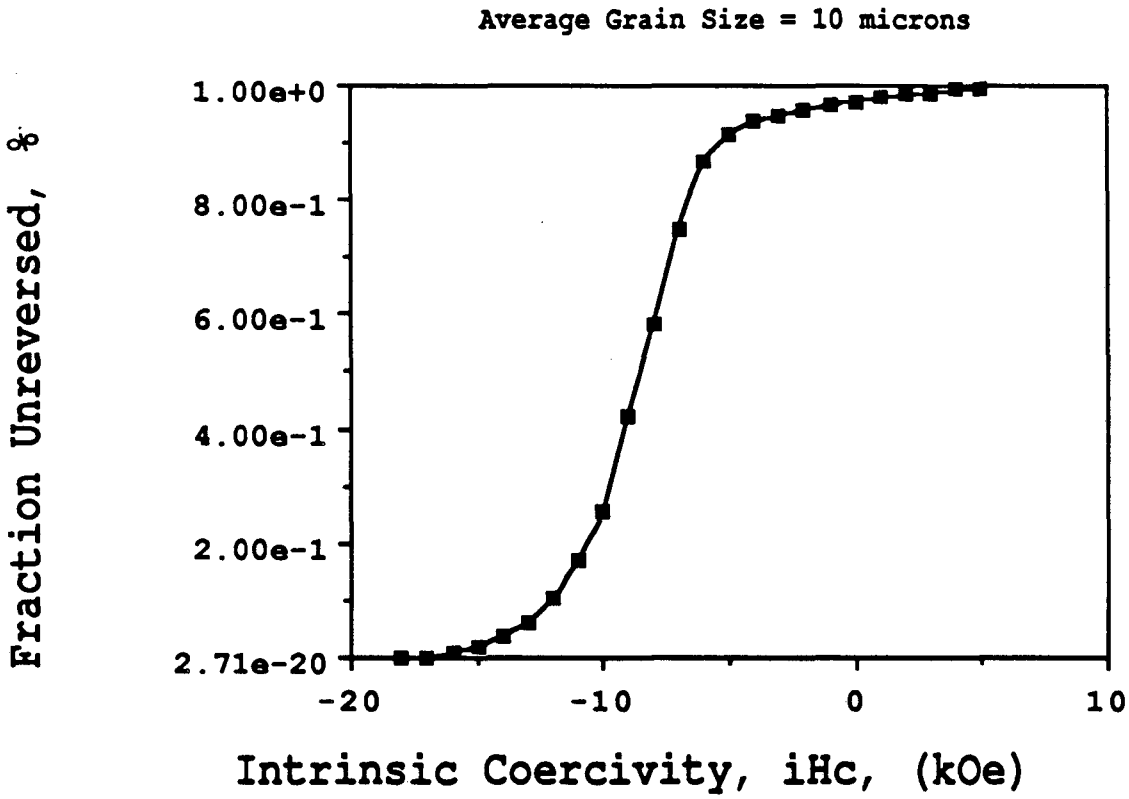

XBL 885-1551

Figure 5

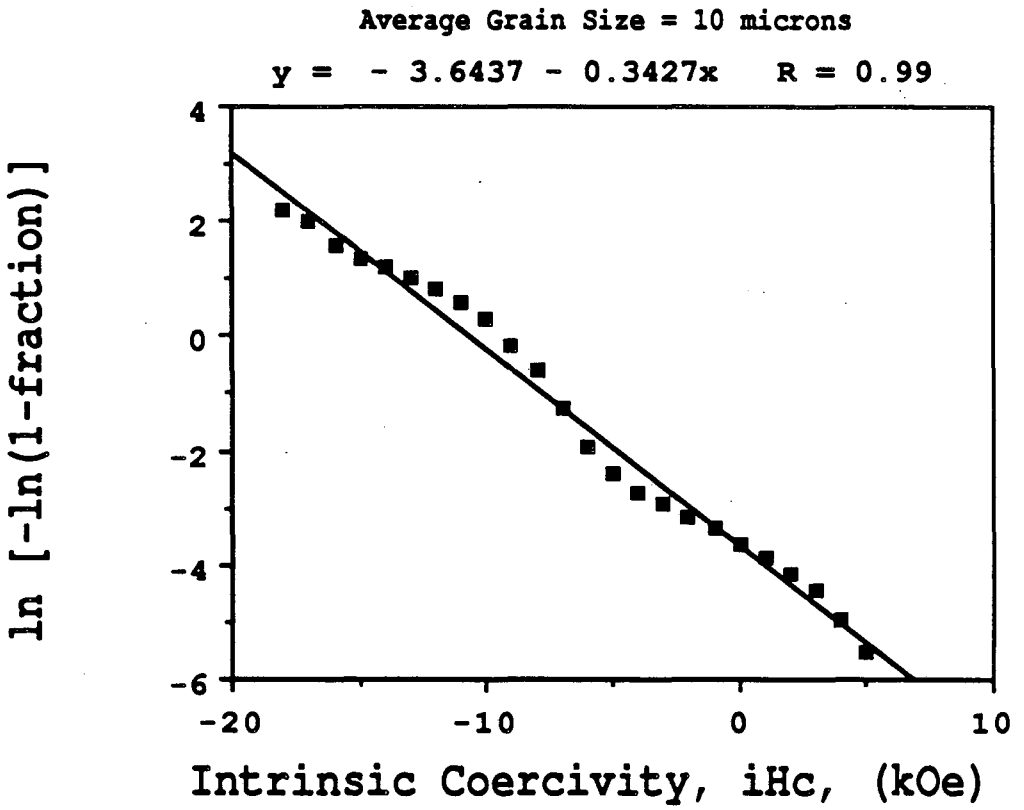

XBL 885-1552

Figure 6

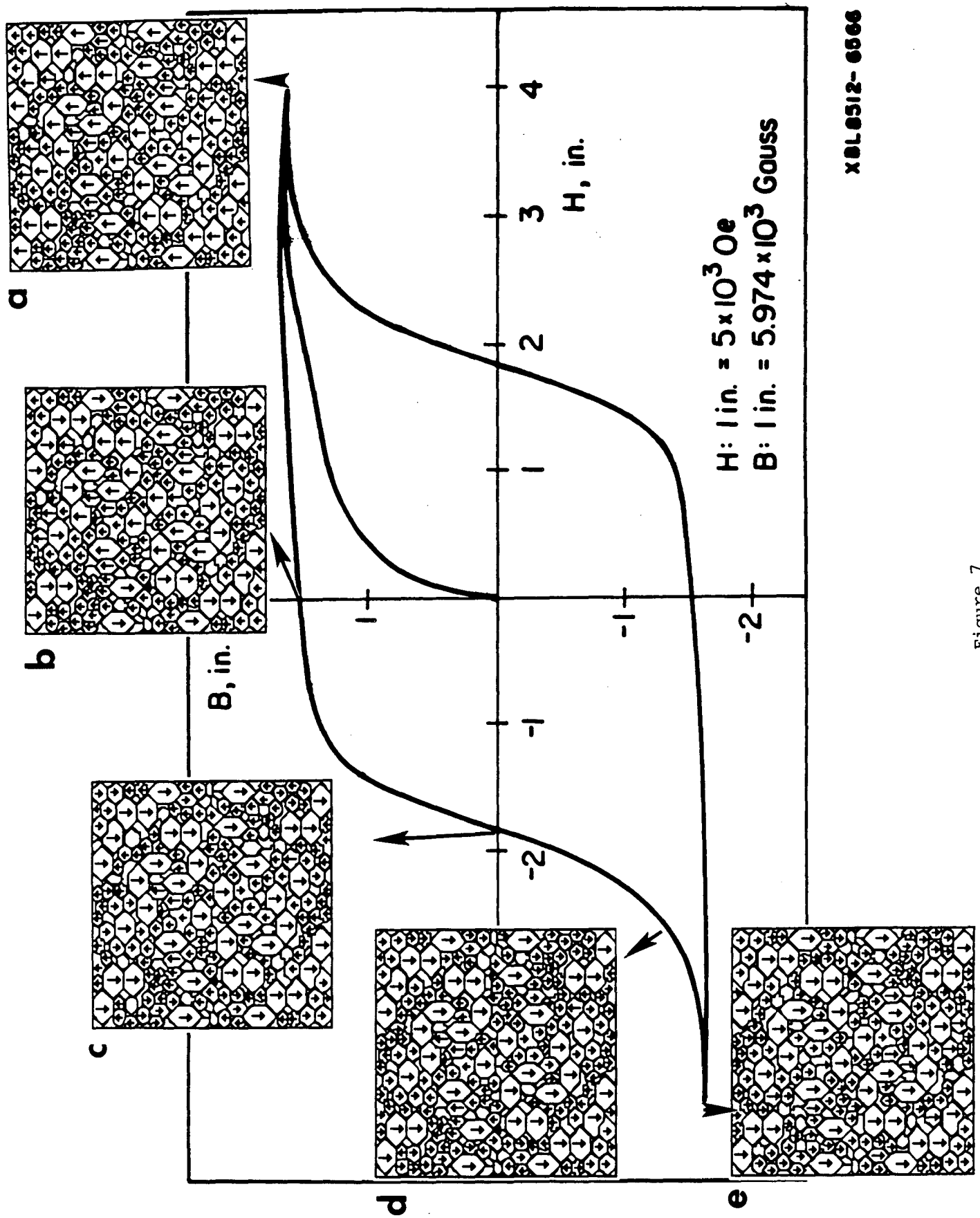
a
b
c
d
e
B, in.
H, in.
1
2
3
4
-1
-2
H: 1 in. = 5x10^3 Oe
B: 1 in. = 5.974x10^3 Gauss
XBL8512-6566

Figure 7

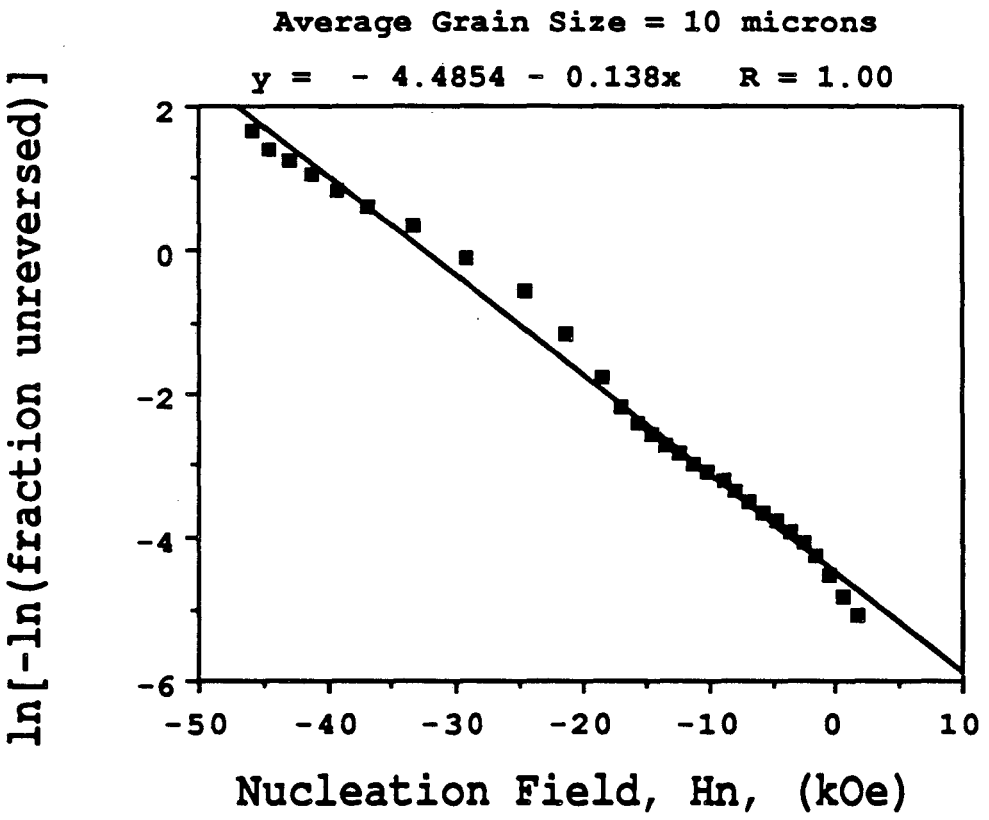

XBB 885 1553

Figure 8

B-H Loop for Polycrystalline Magnets

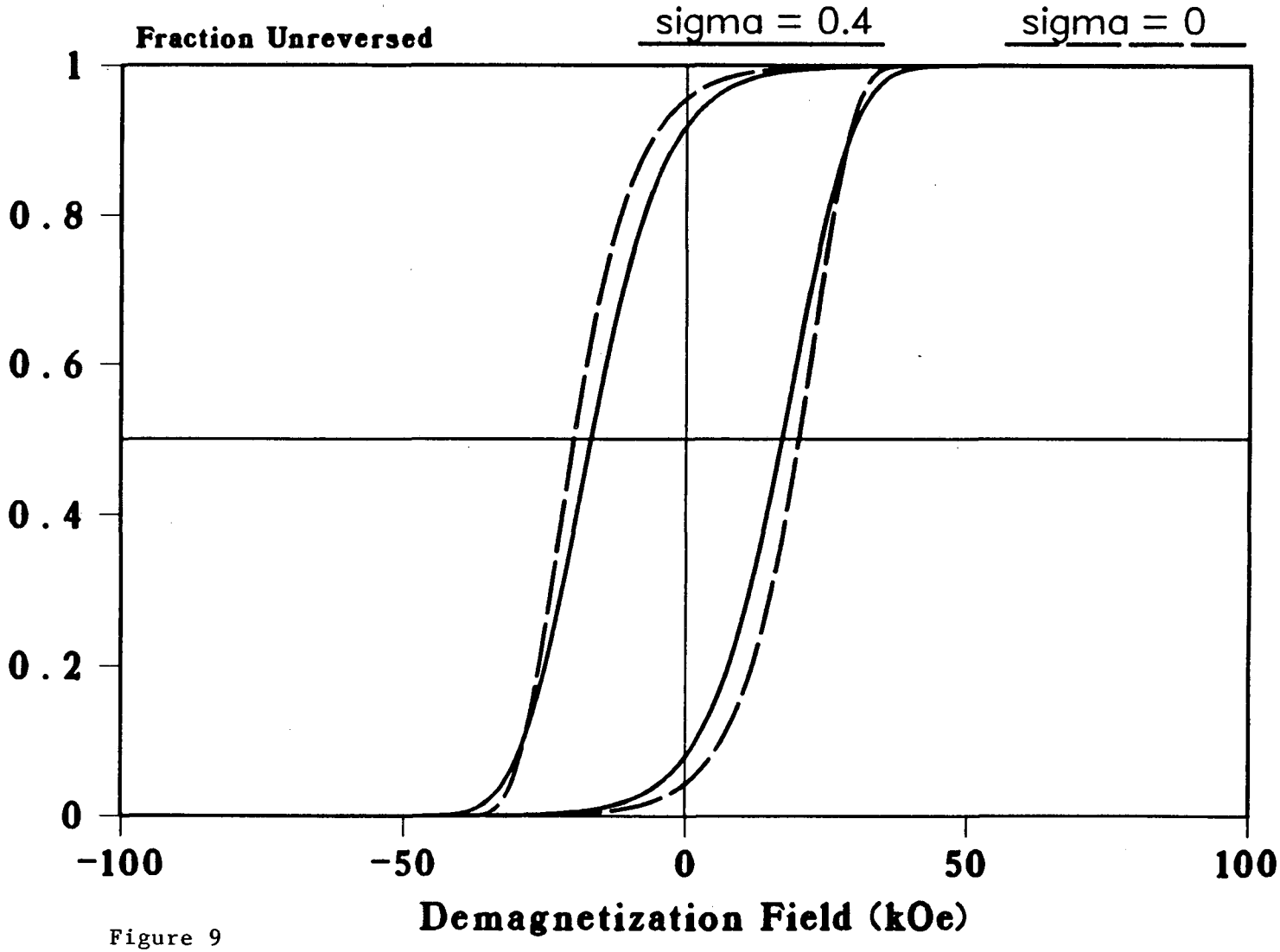

Figure 9

XBL 885 1554

Grain Size Distribution

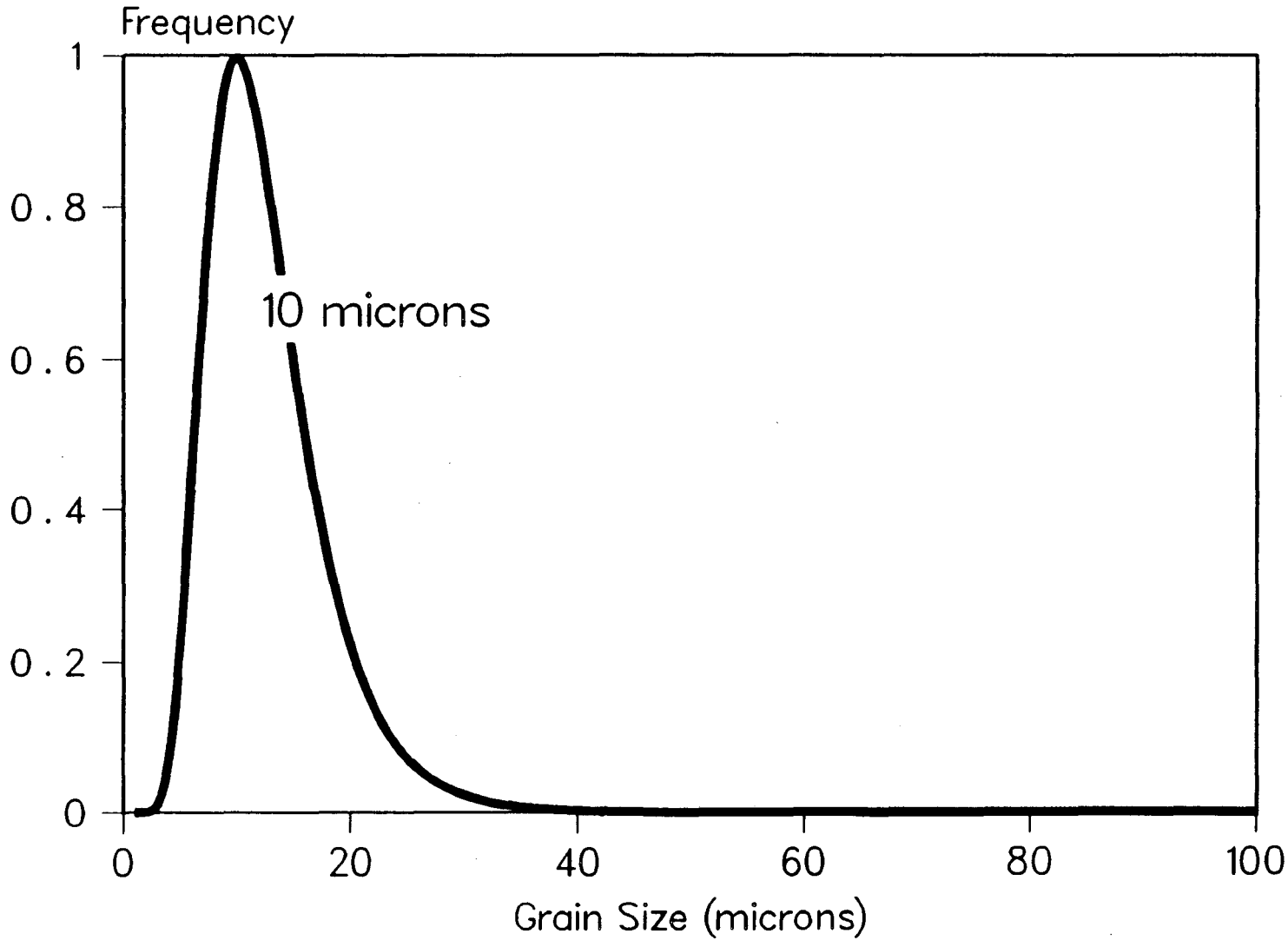

Figure 10

XBL 8710-4520

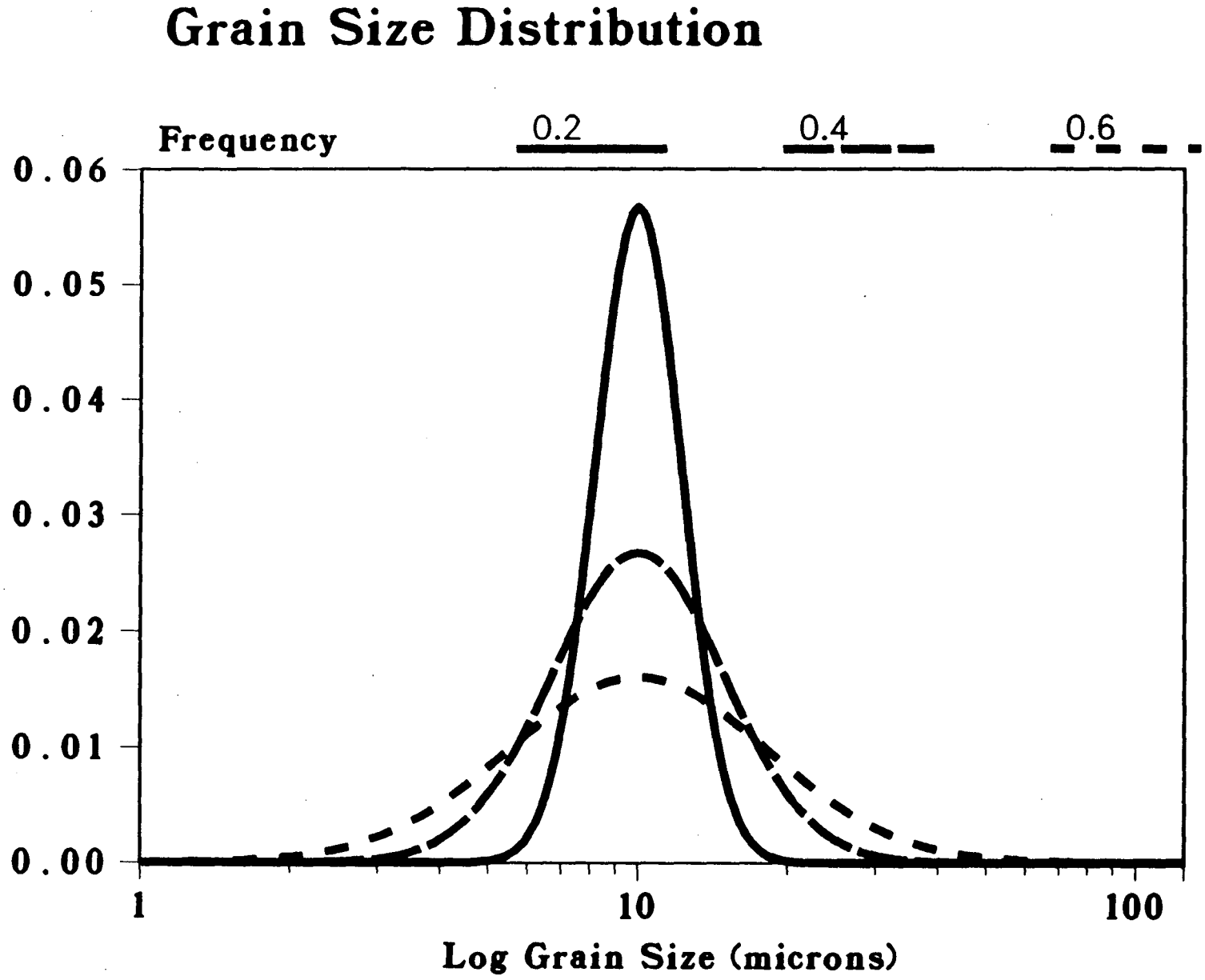

Figure 11

XBL 885 1555

Effect of Standard Deviation on B–H Loop

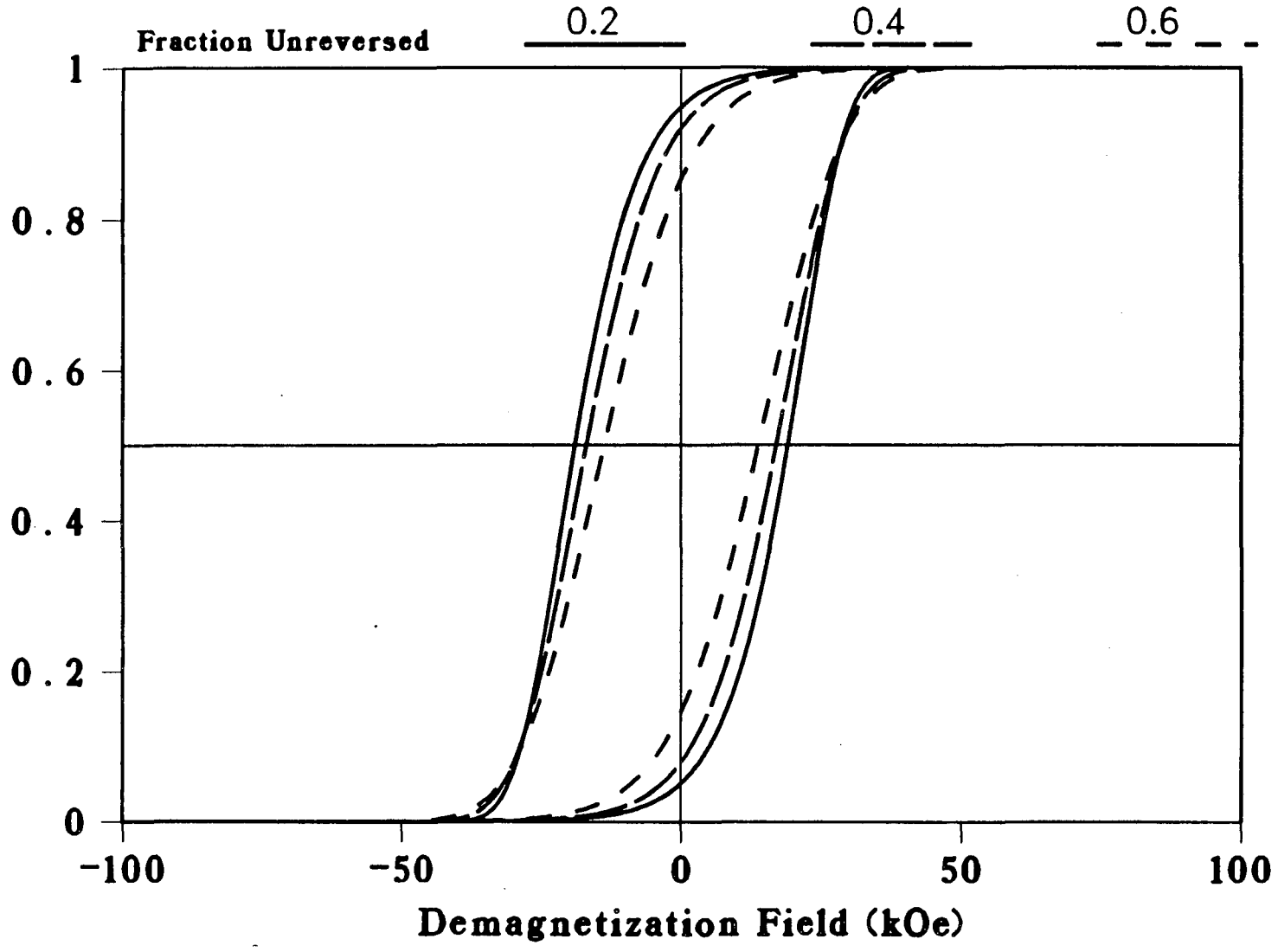

Figure 12

XBL 885 1556

Grain Size Distribution

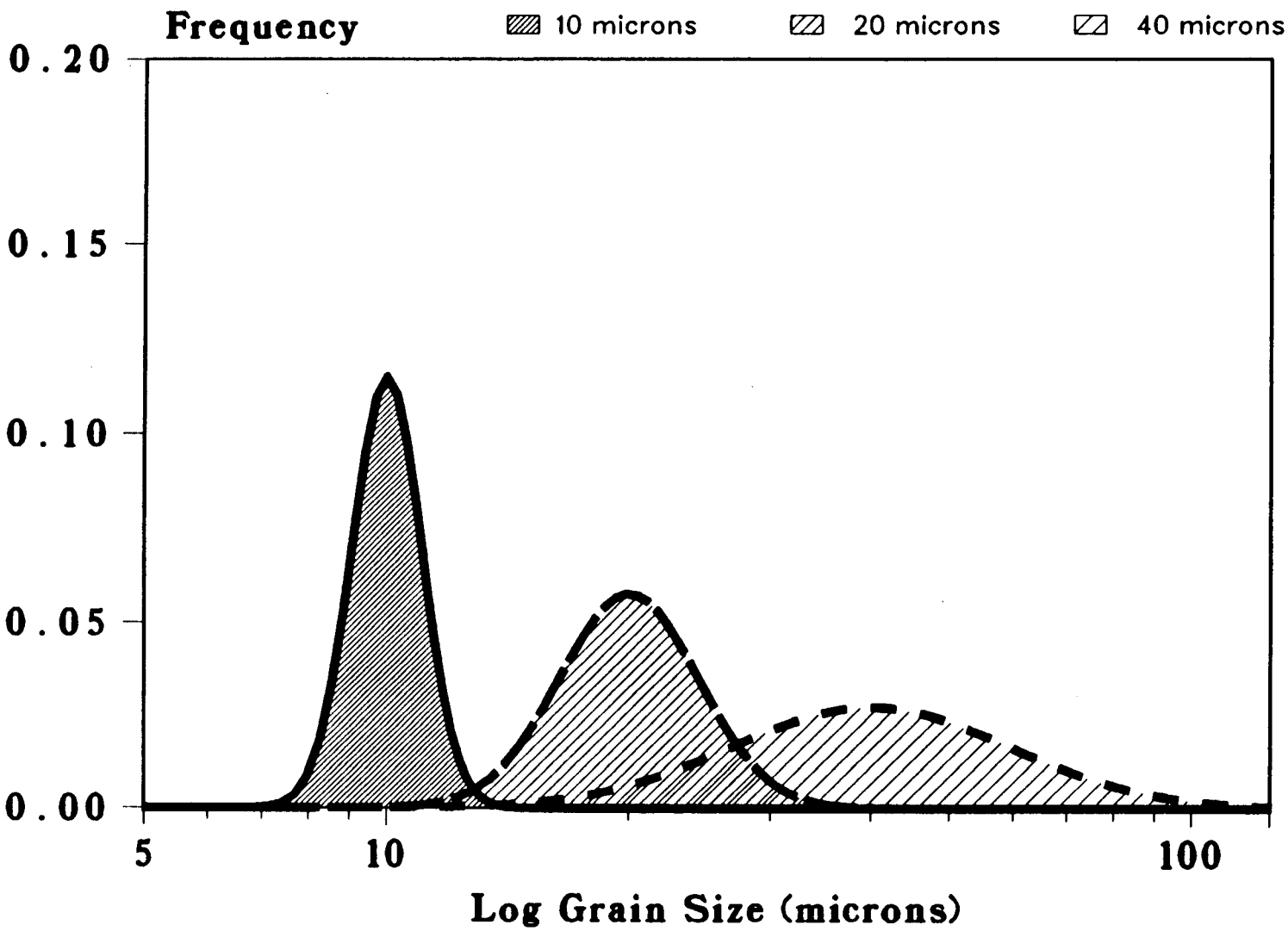

Figure 13

XBL 8711-4612 --

Effect of Grain Size on B-H Loop

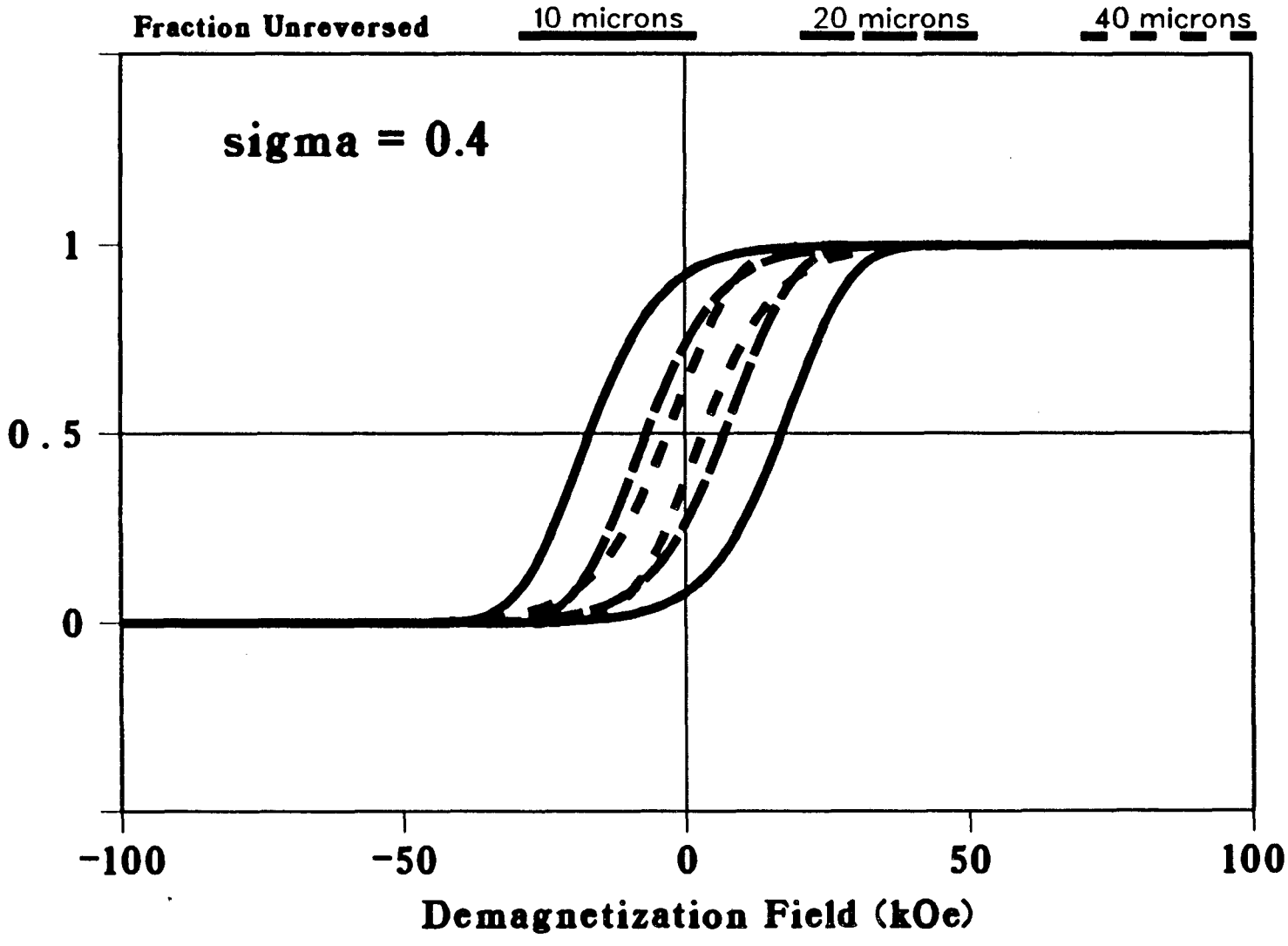

Figure 14

XBL 8711-4613

Effect of Bimodal Distribution

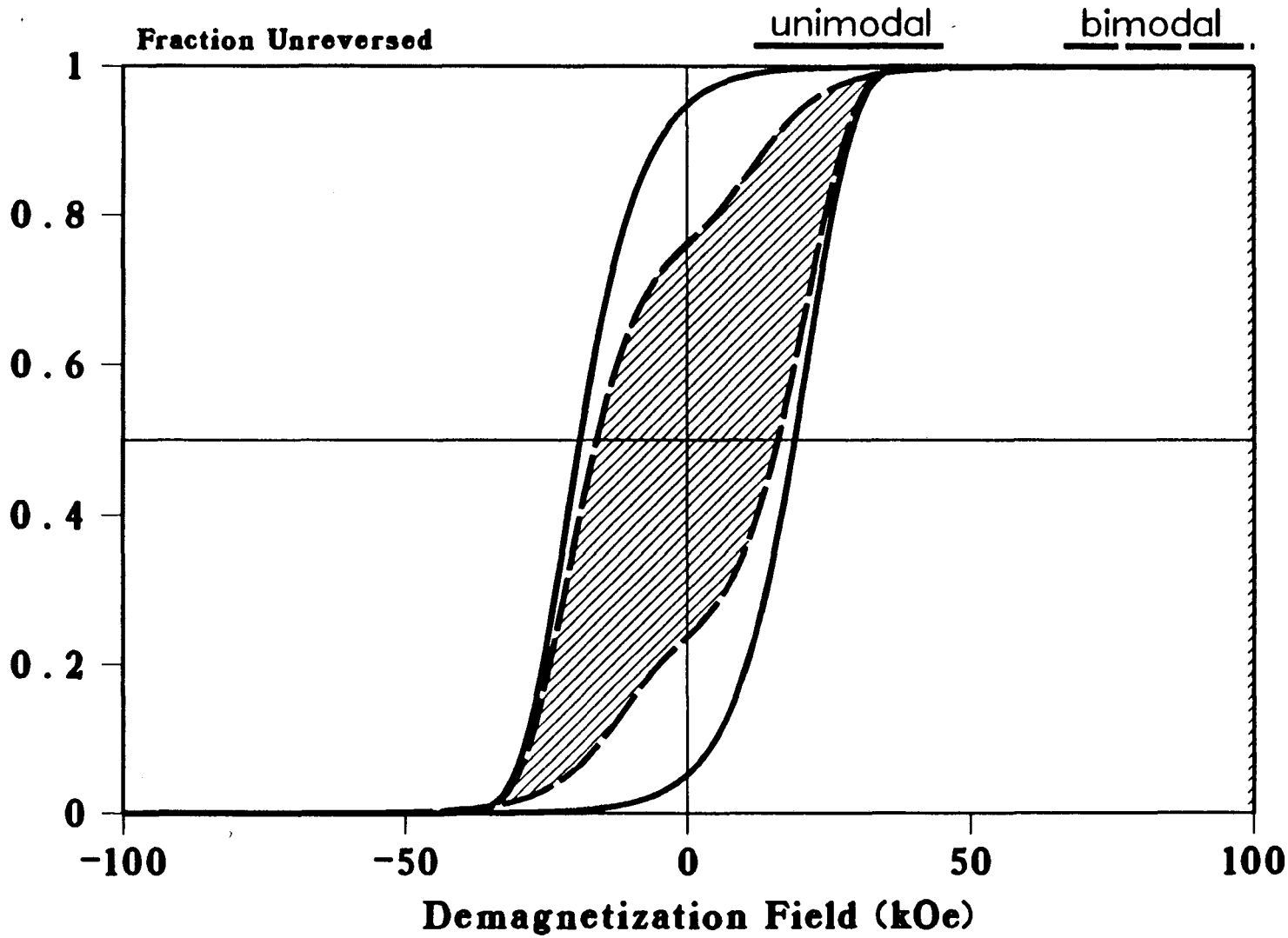

Figure 15

XBL 885 1557

Grain Size Distribution

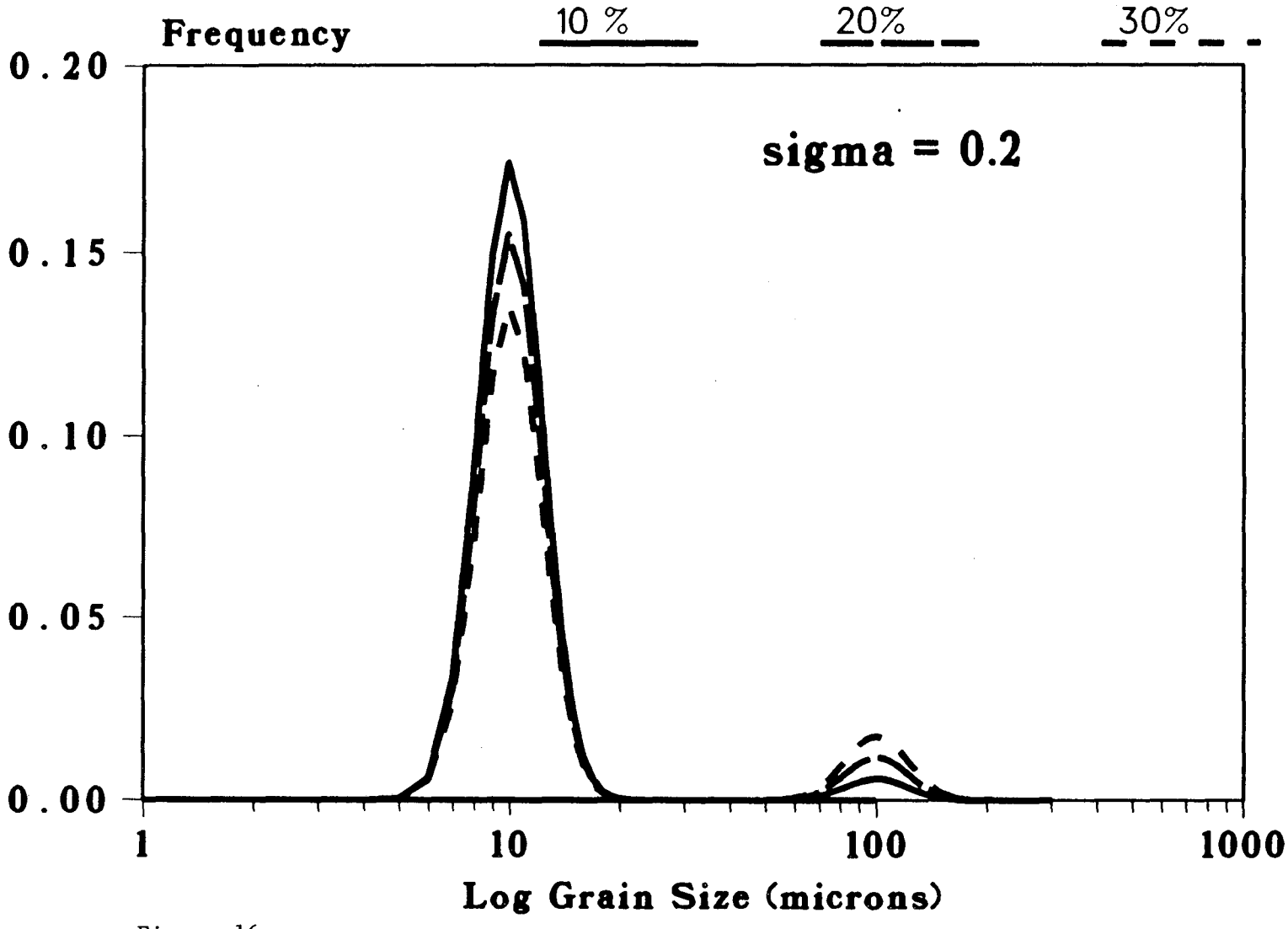

Figure 16

XBL 8711-4610

Effect of Bimodal Distribution on B - H Loop

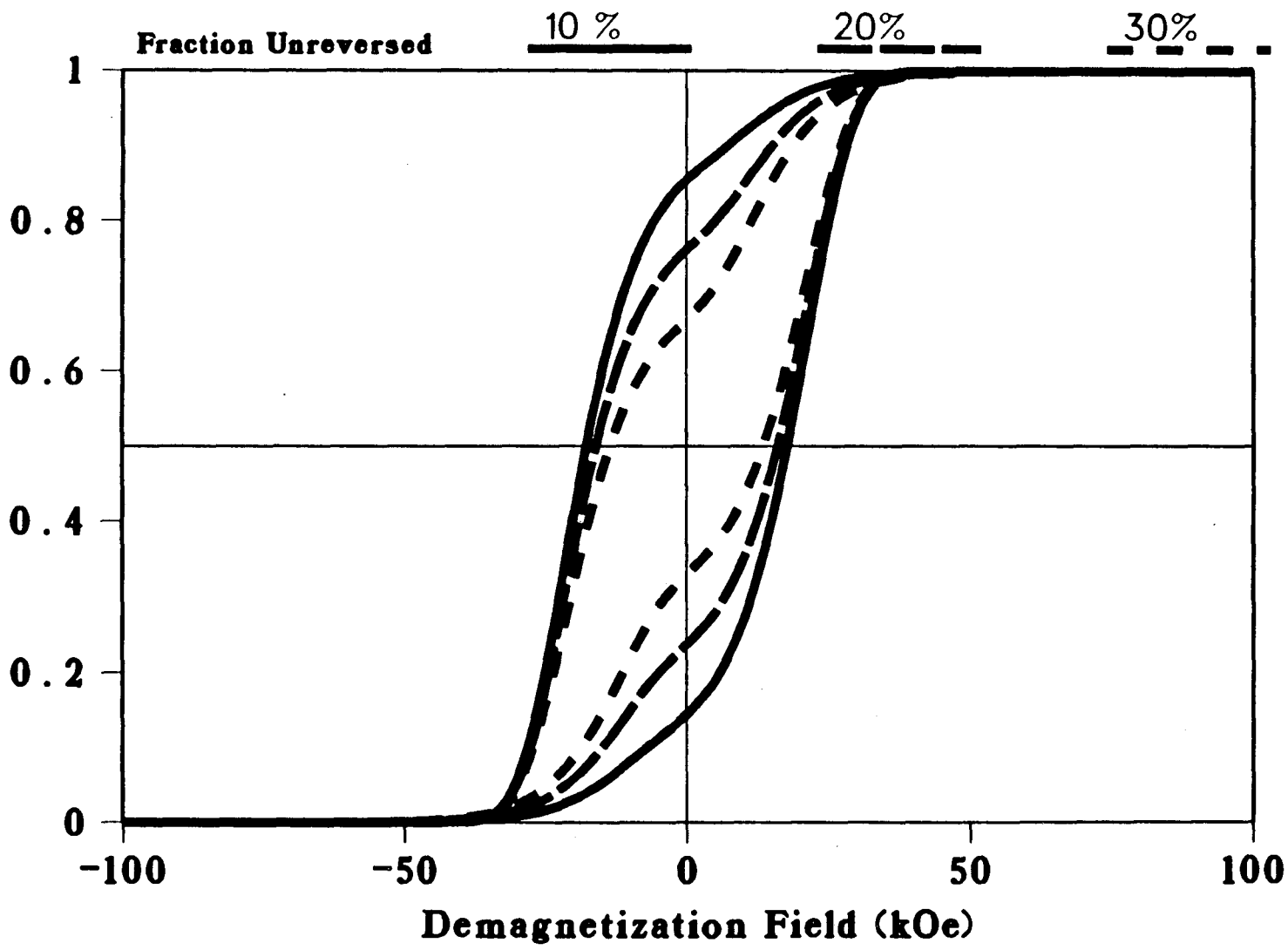

Figure 17

XBL 8711-4611

LAWRENCE BERKELEY LABORATORY
TECHNICAL INFORMATION DEPARTMENT
UNIVERSITY OF CALIFORNIA
BERKELEY, CALIFORNIA 94720